

# RGS14 is a natural suppressor of both synaptic plasticity in CA2 neurons and hippocampal-based learning and memory

Sarah Emerson Lee<sup>a</sup>, Stephen B. Simons<sup>b</sup>, Scott A. Heldt<sup>c,d</sup>, Meilan Zhao<sup>b</sup>, Jason P. Schroeder<sup>e</sup>, Christopher P. Vellano<sup>a</sup>, D. Patrick Cowan<sup>a</sup>, Suneela Ramineni<sup>a</sup>, Cindee K. Yates<sup>a</sup>, Yue Feng<sup>a</sup>, Yoland Smith<sup>f,g</sup>, J. David Sweatt<sup>h</sup>, David Weinschenker<sup>e</sup>, Kerry J. Ressler<sup>c,d,f</sup>, Serena M. Dudek<sup>b</sup>, and John R. Hepler<sup>a,1</sup>

Departments of <sup>a</sup>Pharmacology, <sup>c</sup>Psychiatry and Behavioral Sciences, and <sup>e</sup>Human Genetics, <sup>d</sup>Center for Behavioral Neuroscience, <sup>f</sup>Yerkes National Primate Research Center, and <sup>g</sup>Department of Neurology, Emory University School of Medicine, Atlanta, GA 30322; <sup>b</sup>National Institute of Environmental Health Sciences, National Institutes of Health, Research Triangle Park, NC 27709; and <sup>h</sup>Department of Neurobiology, University of Alabama School of Medicine, Birmingham, AL 35294

Edited\* by Lutz Birnbaumer, National Institute of Environmental Health Sciences, Research Triangle Park, NC, and approved August 17, 2010 (received for review April 19, 2010)

Learning and memory have been closely linked to strengthening of synaptic connections between neurons (i.e., synaptic plasticity) within the dentate gyrus (DG)–CA3–CA1 trisynaptic circuit of the hippocampus. Conspicuously absent from this circuit is area CA2, an intervening hippocampal region that is poorly understood. Schaffer collateral synapses on CA2 neurons are distinct from those on other hippocampal neurons in that they exhibit a perplexing lack of synaptic long-term potentiation (LTP). Here we demonstrate that the signaling protein RGS14 is highly enriched in CA2 pyramidal neurons and plays a role in suppression of both synaptic plasticity at these synapses and hippocampal-based learning and memory. RGS14 is a scaffolding protein that integrates G protein and H-Ras/ERK/MAP kinase signaling pathways, thereby making it well positioned to suppress plasticity in CA2 neurons. Supporting this idea, deletion of exons 2–7 of the RGS14 gene yields mice that lack RGS14 (RGS14-KO) and now express robust LTP at glutamatergic synapses in CA2 neurons with no impact on synaptic plasticity in CA1 neurons. Treatment of RGS14-deficient CA2 neurons with a specific MEK inhibitor blocked this LTP, suggesting a role for ERK/MAP kinase signaling pathways in this process. When tested behaviorally, RGS14-KO mice exhibited marked enhancement in spatial learning and in object recognition memory compared with their wild-type littermates, but showed no differences in their performance on tests of nonhippocampal-dependent behaviors. These results demonstrate that RGS14 is a key regulator of signaling pathways linking synaptic plasticity in CA2 pyramidal neurons to hippocampal-based learning and memory but distinct from the canonical DG–CA3–CA1 circuit.

long-term potentiation | hippocampus | G protein signaling | RGS proteins | ERK

Many aspects of brain plasticity, including those associated with learning and memory, are thought to be mediated by long-term potentiation (LTP) of excitatory glutamatergic synaptic transmission (1). Plasticity at synapses of the DG–CA3–CA1 circuit within the hippocampus, in particular, plays a key role in acquisition and consolidation of certain forms of learning and memory (2, 3). Absent from this canonical DG–CA3–CA1 circuit is the CA2 region, which differs from these regions by its distinct anatomy, pattern of gene expression, and electrophysiological characteristics (4–8). CA2 pyramidal neurons also are uniquely resistant to injury in several animal models of epilepsy and hypoxia but exhibit a unique pathology in brains from schizophrenic patients (9–11). Unexplained, however, is the fact that protocols typically effective at inducing LTP in hippocampal CA1/CA3 subfields are largely ineffective in CA2 neurons at Schaffer collateral synapses (7).

Cellular signaling underlying LTP and synaptic plasticity includes key mechanistic roles for calcium, Ras/MAP kinases, and

G protein signaling pathways (12) among others. The regulators of G protein signaling (RGS) proteins are a structurally diverse family of greater than 30 member proteins enriched in brain that typically limit neurotransmitter receptor- and G protein-linked signaling in the CNS and elsewhere by serving as GTPase activating proteins (GAPs) (13, 14). One particular family member, RGS14, is uniquely situated to regulate signaling pathways involved with synaptic plasticity. Originally identified as a binding partner for Rap GTPases (15, 16), RGS14 has binding domains for multiple signaling proteins including active G $\alpha$ i/o–GTP (RGS domain), Ras/Rap GTPases [tandem Ras Binding Domains (RBDs)] and for inactive G $\alpha$ i1–GDP and G $\alpha$ i3–GDP [a single G protein Regulatory (GPR) motif] (15–20). Most recently, we have shown that RGS14 can act as a scaffold to assemble G $\alpha$ i, H-Ras, and Raf kinases, in turn, to integrate G protein and ERK/MAPK signaling pathways and inhibit growth factor receptor signaling (21). Here we have tested the idea that RGS14 serves to regulate synaptic plasticity in the brain, perhaps with a resulting role in learning and memory.

## Results

RGS14 protein is expressed most prominently in brain, and exclusively within neurons (18). To better understand the role of RGS14 in brain function, we determined its protein distribution pattern in mouse brain sections using a specific anti-RGS14 monoclonal antibody. We observe that RGS14 exhibits a striking expression pattern with strong immunohistochemical staining that is mostly limited to the CA2 subregion of the hippocampus (Fig. 1*A* and *B*); light staining is also seen in the olfactory cortex. This protein staining pattern very closely matches the mRNA distribution pattern of RGS14 in mouse brain (<http://mouse.brain-map.org>; Fig. S1). The staining is completely eliminated by pre-adsorption of antibody with purified RGS14 protein (Fig. 1*C*). Within the hippocampus, strong immunoreactivity is evident in soma and neurites of CA2 pyramidal neurons that appear to project through the stratum lacunosum moleculare and stratum radiatum to the fasciola cinerea (FC) (Fig. 1*B* and *D*). Within the FC, strong staining is evident in pyramidal neurons in soma and neurites (Fig. 1*F*). With this finding, RGS14 joins a discrete fraternity of signaling proteins that share this highly restricted expression pattern in both

Author contributions: S.E.L., J.P.S., Y.F., Y.S., J.D.S., D.W., K.J.R., S.M.D., and J.R.H. designed research; S.E.L., S.B.S., S.A.H., M.Z., C.P.V., D.P.C., S.R., and C.K.Y. performed research; S.E.L., S.B.S., M.Z., S.A.H., and J.P.S. analyzed data; and S.E.L., S.M.D., and J.R.H. wrote the paper.

The authors declare no conflict of interest.

\*This Direct Submission article had a prearranged editor.

<sup>1</sup>To whom correspondence should be addressed. E-mail: jhepler@pharm.emory.edu.

This article contains supporting information online at [www.pnas.org/lookup/suppl/doi:10.1073/pnas.1005362107/-DCSupplemental](http://www.pnas.org/lookup/suppl/doi:10.1073/pnas.1005362107/-DCSupplemental).

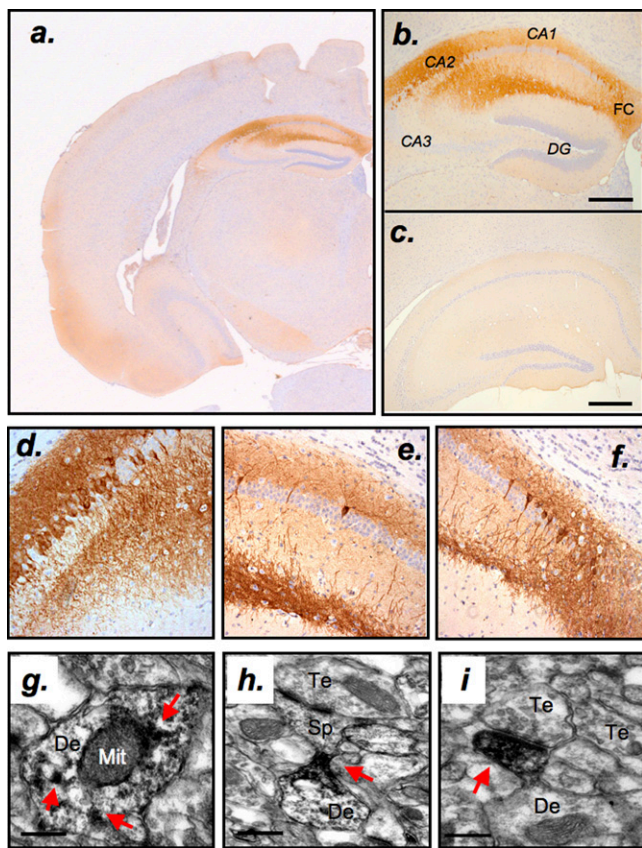


**Fig. 1.** RGS14 is enriched in hippocampal CA2 neurons. (A and B) Fixed paraffin-embedded mouse brain sections stained with anti-RGS14 monoclonal antibody (brown, DAB staining with specific anti-RGS14 monoclonal antibody) and counterstained with hematoxylin (blue). (C) Elimination of RGS14 staining by preadsorption of antibody with purified recombinant RGS14 protein. (Scale bar, 400  $\mu$ m.) (D) RGS14 expression in CA2 neurons, (E) in a discrete subset of CA1 neurons, and (F) in neurons within the fasciola cinerea (FC). (G–I) Electron micrographs of RGS14-immunoreactive (red arrows). (G) Dendritic shaft (de), (H) spine (sp) neck, and (I) spine head in the stratum oriens region of mouse CA2 hippocampus. (Scale bar, 0.2  $\mu$ m.) DAB staining with RGS14 antibody. Other recognized structures are mitochondria (mit).

CA2 and FC neurons (6), suggesting a possible functional link between these proteins and these two poorly understood hippocampal regions. Staining is also observed in soma and neurites of sporadic, unidentified neurons within the CA1 pyramidal cell layer, which we speculate to be either inhibitory interneurons or a distinct subset of pyramidal neurons (Fig. 1E). At the electron microscopic (EM) level, RGS14 labeling in CA2 hippocampal neurons is predominantly found in dendritic shafts (Fig. 1G), as well as necks or heads of dendritic spines (Fig. 1H and I), including an apparent enrichment at some postsynaptic densities (PSD) (Fig. 1I). This conspicuous distribution pattern of RGS14 within the hippocampus highlights the divergent molecular nature and anatomical circuitry of neurons in the CA2 and suggests that CA2 functions may be distinct from those of the neighboring CA1 and CA3 regions.

To determine RGS14 functions in brain and hippocampal physiology, we characterized a novel line of knockout mice lacking full-length RGS14 (RGS14-KO) generated by inserting a LacZ/Neo cassette that deletes exons 2–7 of the RGS14 gene (<http://www.informatics.jax.org>) (Fig. S2). As shown in Fig. 2, PCR analysis of genomic DNA shows loss of the wild-type (WT) gene in RGS14-KO mice, and the presence of the targeting vector (Fig. 2A Upper). RT-PCR analysis of mRNA shows loss of RGS14 message (Fig. 2A Lower and Fig. S2). Immunoblot analysis of

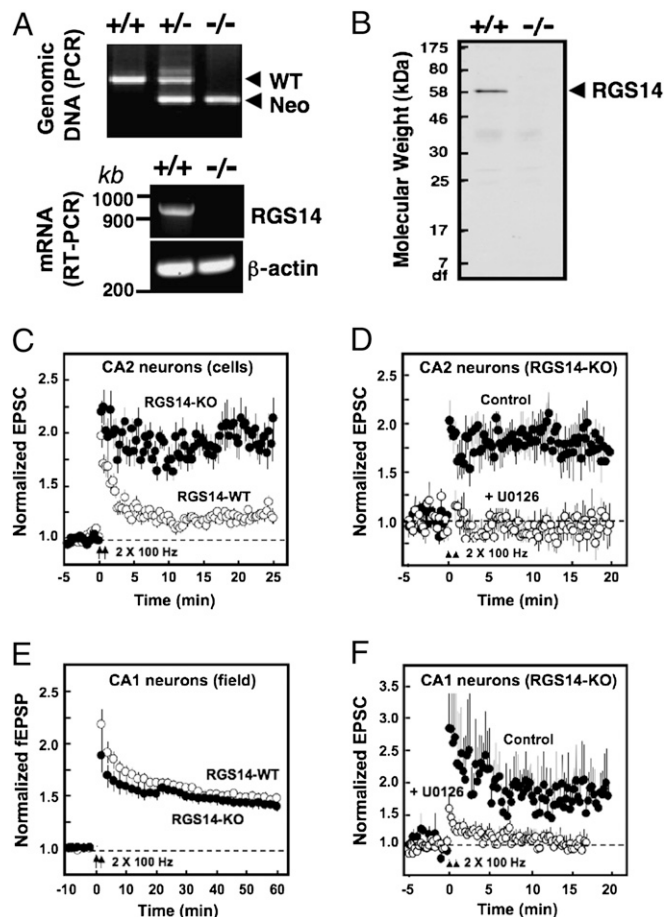


**Fig. 2.** Loss of RGS14 allows for induction of nascent LTP in CA2 neurons following high-frequency stimulation that is blocked by a specific MEK inhibitor. (A Upper) PCR genotyping. Multiplex PCR shows single larger band for wild-type (WT) genomic DNA, two bands for heterozygous RGS14(+/-) genomic DNA, and a single lower band for knockout RGS14(+/-) (RGS14-KO) genomic DNA, indicating loss of RGS14 gene and insertion of lacZ/neo cassette. (A Lower) RT-PCR analysis of RGS14 mRNA. No mRNA product seen for any of the RT-PCR primers used in RGS14-KO. (B) Protein immunoblot for RGS14 protein using a specific anti-RGS14 monoclonal antibody. Lane 1, WT RGS14 (+/+) brain lysates; lane 2, RGS14-KO brain lysates. (C) For induction of LTP, CA2 neurons were stimulated ( $2 \times 1$  s, 100 Hz, 20-s intervals) and excitatory postsynaptic currents (EPSCs) measured WT ( $n = 5$  mice, 22 neurons) and RGS14-KO ( $n = 6$  mice, 24 neurons). Plotted are means  $\pm$  SEM. (D) For inhibition of LTP in CA2 neurons by treatment with a MEK inhibitor, experiments on individual CA2 neurons from RGS14-KO mice were performed as in C except that 500 nM U0126 was included in the bath solution ( $n = 7$  with U0126 and  $n = 9$  without). Plotted are means  $\pm$  SEM. (E) For induction of LTP in CA1, hippocampal slices from WT and RGS14-KO mice were stimulated ( $2 \times 1$  s, 100 Hz, 20-s intervals) and postsynaptic neurotransmission was monitored every 15 s for 180 min. Data are pooled (mean  $\pm$  SD); WT ( $n = 10$ ), RGS14-KO ( $n = 8$ ). (F) For inhibition of LTP in CA1 neurons by treatment with a MEK inhibitor, experiments on individual CA1 neurons from RGS14-KO mice were performed as in C except that 500 nM U0126 was included in the bath solution ( $n = 7$  with U0126 and  $n = 4$  without). Plotted are means  $\pm$  SEM.

mouse brain lysates shows RGS14 as a single band of expected molecular weight (60 kDa) in WT brain and no corresponding band in RGS14-KO brain lysates (Fig. 2B), indicating complete loss of full-length protein. RGS14-KO mice appear healthy with no obvious differences in their growth, fertility, or any apparent physiological phenotype compared with their wild-type and heterozygous littermates.

Because RGS14 is expressed primarily in CA2 hippocampal neurons, we tested the effects of loss of RGS14 on synaptic transmission in CA2 compared with CA1 neurons (Fig. 2C–F). In

rodents, high-frequency synaptic stimulation (HFS) in the stratum radiatum results in a sustained marked enhancement of post-synaptic responses—i.e., LTP—in CA1 and CA3 neurons (22). However, CA2 neurons differ from their neighboring neurons by their curious lack of plasticity following synaptic stimulation to Schaffer collateral synapses (7). We discovered that the loss of RGS14 confers to CA2 neurons a robust capacity for this type of plasticity (Fig. 2C), whereas CA2 neurons from wild-type animals exhibited little LTP following HFS as expected. On the other hand, both the RGS14-KO and WT mice displayed normal LTP in CA1 neurons assessed in field potentials (Fig. 2E). The basal synaptic transmission in CA2 and CA1 neurons was also normal in both WT and KO animals (Fig. S3). Hence, RGS14 may act as a natural brake to limit synaptic plasticity within the CA2 following stimulation.

We next investigated possible underlying molecular mechanisms to explain how losing RGS14 enhances synaptic plasticity in CA2 neurons. RGS14 binds Rap2, G $\alpha$ 1/3-GDP, H-Ras, and Raf kinases to inhibit growth factor-directed MAP kinase signaling (16, 21, 23). Therefore, we tested whether treatment of CA2 neurons with a specific inhibitor of ERK/MAP kinase signaling affected the increased capacity for LTP caused by the loss of RGS14. We find that the MEK inhibitor U0126 completely prevented this robust LTP induction in CA2 neurons (Fig. 2D), thus implicating RGS14 as a suppressor of MAP kinase signaling in this process. The MEK inhibitor also blocked LTP in CA1 neurons (Fig. 2F), as expected (24), suggesting a key role for MEK/ERK signaling in the regulation of LTP in both CA2 and CA1 neurons. This effect of the MEK inhibitor on LTP in CA2 neurons does not rule out a possible additional role for G protein signaling and regulation of potassium channel function. Consistent with evidence that MAPK or G protein signaling can influence neuronal excitability (25–28), we also observed that loss of RGS14 results in a modest increase in input resistance in CA2 neurons (Fig. S4A and B), which could be due to loss of regulation of either RGS14 binding partner H-Ras or G $\alpha$ i. This concomitant increase in neuronal excitability, however, is not sufficient to substantially impact the action potential response to high-frequency stimulation (Fig. S4C). Taken together, these findings support our hypothesis that RGS14 serves as a previously unknown natural suppressor of signaling pathways important for LTP in CA2 neurons.

Because RGS14-KO mice exhibited markedly enhanced synaptic plasticity in CA2 neurons, we hypothesized that hippocampal-based spatial learning and memory in RGS14-KO mice might also be enhanced (Fig. 3). To test this idea, we first measured declarative memory using a novel object recognition task (29). Mice were allowed to explore two identical objects. Four and 24 h later one object was replaced with a novel object to test for signs of object recognition. Although both groups of mice showed similar baseline exploratory behavior by spending an equivalent amount of time with the identical objects, after 4 h, RGS14-KO mice spent significantly more time than WT mice exploring (Fig. 3A) and made more contacts with the novel object in the test trials (Fig. 3B), indicating enhanced recognition memory. Of note, our findings here are inconsistent with a recent report that shows overexpression of RGS14 in the visual cortex enhances novel object recognition (30). Because those studies involved overexpression of recombinant RGS14 in a brain region where it is not naturally expressed, we believe our findings more accurately reflect the physiological role for RGS14 in the context of novel object recognition.

In a second test of hippocampal function, we subjected mice to the Morris water maze (MWM) to test for spatial learning. In this task, rodents navigate a swim arena using visual cues to locate a submerged escape platform (31). In repeated trials of the MWM, paired WT and RGS14-KO littermates showed a similar latency to escape on day 1, and exhibited typical learning behavior improving each day, reaching a plateau by day 5. Surprisingly however, RGS14-KO animals exhibited a significantly enhanced initial learning rate that was sustained each day (Fig. 3C). In probe

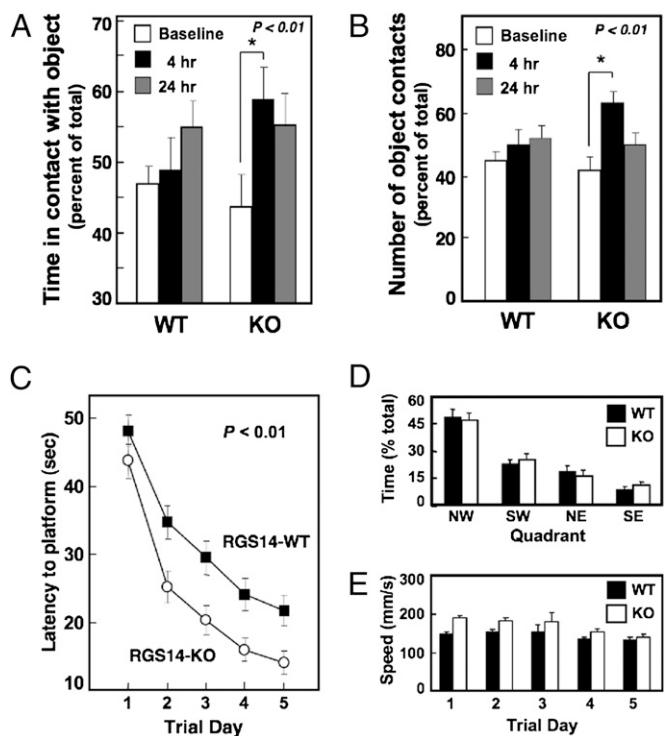


**Fig. 3.** Loss of RGS14 enhances hippocampal-based spatial learning and object working memory. (A and B) Novel object recognition task: (A) Percentage of total time spent exploring and (B) percentage of total contacts made on two objects for 5 min during training, and memory for object at 4 and 24 h after training (paired *t* test, \**P* < 0.01; *n* = 34, WT; *n* = 20, RGS14-KO). (C) Morris water maze task: latency for WT and RGS14-KO mice to reach a hidden platform in acquisition trials over 5 d (two factor, repeated measures ANOVA; \**P* < 0.01). (D) Probe trial on day 6 for WT and RGS14-KO mice; time spent in each quadrant with escape platform removed. (E) Average swim speed over 5 d of acquisition training (C–E: *n* = 17, WT; *n* = 16, RGS14-KO).

trials after 6 d of testing, the platform was removed to determine whether the animals would perseverate in their search for the platform in the previous location. WT and RGS14-KO mice spent more (and similar amounts of) time in the trained quadrant (Fig. 3D), indicating that both groups learned the platform location. Differences in behavior were limited to those tasks linked to the hippocampus, as both groups swam at similar speeds (Fig. 3E), and we observed no differences in ambulatory behavior (Fig. S5A), baseline startle response, sensory-motor gating (Fig. S5B and C), or anxiety in the elevated plus maze (Fig. S5D). These altered behaviors coupled with the observed enhancement of CA2-specific plasticity of postsynaptic transmission in RGS14-KO animals indicate that the presence of RGS14 limits hippocampal-based learning and memory.

## Discussion

Very little is known about the role of the CA2 subregion in hippocampal function and behavior. CA2 synapses are unusually stable and resistant to plasticity (LTP) following typical modes of stimulation (7). No previous studies implicate a role for the CA2 in spatial learning or memory except that it may be involved in social recognition memory and memory for temporal order (32). Yet, we show here that the loss of RGS14, a single CA2-enriched gene, abrogates this synaptic stability resulting in both robust LTP in CA2 neurons and an enhancement of spatial learning and object recognition memory. Only a few signaling proteins that could contribute to its unusually weak LTP have been reported to be localized in CA2 neurons (6, 8), and possible roles for those

proteins (if any) in synaptic plasticity have not been defined. By contrast, many signaling proteins and pathways have been implicated in the positive regulation of LTP, synaptic plasticity, and learning and memory in other, non-CA2 hippocampal regions (1, 33). Among them are the identified RGS14 binding partners G $\alpha$ i1, active H-Ras and Rap2, and associated MAP kinase signaling pathways (12).

At present, the exact molecular mechanism by which RGS14 regulates LTP in CA2 neurons remains uncertain. Our findings here show that loss of RGS14 results in nascent LTP that is prevented by inhibiting MEK (Fig. 2), indicating that RGS14 may be acting as a natural suppressor of ERK1/2 signaling pathways underlying synaptic plasticity. Consistent with this idea, we have shown that RGS14 integrates G protein and H-Ras/Raf signaling to inhibit growth factor stimulated ERK1/2 signaling (21). We also find that RGS14 is localized at dendritic spines (Fig. 1D) and may be enriched in Triton-X 100 insoluble postsynaptic densities (18), i.e., well-established focal points for synaptic plasticity-related signaling. RGS14 binding partners H-Ras and Rap2 modulate the activity of various MAP kinase pathways in hippocampal neurons (34) and have been implicated in different aspects of LTP and synaptic plasticity in the hippocampus (34–41). However, RGS14 also binds Gi/o family members at both the GPR domain and the RGS domain, and our findings do not rule out a possible role for RGS14 regulation of Gi/o protein signaling in this process. G $\beta$  $\gamma$  subunits derived from Gi/o regulate certain potassium and calcium channels in brain, and the G protein-regulated second messengers cAMP and calcium each play crucial roles in learning, memory, and synaptic plasticity by regulating gene expression and modulating postsynaptic signaling events (22, 42). Thus, loss of RGS14 and with it, its capacity to limit G $\alpha$ i/o signaling, may alter postsynaptic cAMP and/or calcium levels to enhance LTP and learning. Further studies are necessary to determine the role for each of these binding partners and their linked signaling pathways in RGS14-mediated suppression of synaptic plasticity in CA2 neurons.

In summary, RGS14 is a natural suppressor of signaling pathways critically involved with regulating synaptic plasticity, and its host CA2 neurons may represent a newly recognized module that functions either distinct from, or in concerted action with the canonical trisynaptic circuit to mediate hippocampal-based learning and memory. Given the very discrete protein expression pattern of RGS14 and the fact that RGS14-KO mice exhibit no obvious deleterious phenotypes, inhibition of RGS14 function may serve as an attractive therapeutic target for future cognitive enhancers (43, 44).

## Materials and Methods

**Generation, Genotyping, and RT-PCR of RGS14-KO Mutant Mice.** Mice lacking RGS14 (RGS14<sup>tm1-lex</sup>) were generated by Lexicon Genetics through the National Institutes of Health-sponsored Mutant Mouse Regional Resource Center at [http://www.informatics.jax.org/searches/accession\\_report.cgi?id=MGI:3528963](http://www.informatics.jax.org/searches/accession_report.cgi?id=MGI:3528963). Embryos were implanted into C57/BL6 females, and founder mice crossed with C57/BL6 to establish the novel knockout line (RGS14-KO). Genotypes were determined by PCR of genomic DNA from tail biopsies. WT forward primer was 5' cagcgcctcgtctctatc 3'. Primer for the targeting vector was 5' gcagcgcctcgtctctatc 3' with a shared reverse primer (5' agactggcagaagaattcagg 3'). PCR reactions were performed with Platinum Taq (Invitrogen) under the following amplification conditions: 94 °C for 3 min, and 30 cycles of 94 °C for 30 s, 64 °C for 30 s, 72 °C for 45 s, and completing with 72 °C for 1.5 min. For reverse transcription-PCR (RT-PCR), mRNA from brain tissue of WT and RGS14-KO animals was isolated using Invitrogen PureLink kit with forward (1: 5' caaatccccctgtaccaagagtg 3'; 3: 5' acttgggtgtcccaacggcg 3') and reverse (2: 5' gaagcctgtccgtcaggtagata 3'; 4: 5' gaacatctctgcccgggctgg 3') primers.

**Isolation of Brain Tissue and Immunoblot Analysis.** Before all surgical procedures for histology, mice were deeply anesthetized with isoflurane or with a mixture of ketamine (60–100 mg/kg, i.p.) and dormitor (0.1 mg/kg, i.p.). Brain tissue was harvested following transcardial perfusion of anesthetized mice with cold saline. Lysates were prepared as described (18), subjected to SDS/PAGE, and transferred to nitrocellulose membranes. Membranes were blocked

for 1 h and incubated overnight with a specific anti-RGS14 mouse monoclonal antibody (Antibodies, Inc.), washed, and then probed with horseradish peroxidase-conjugated goat anti-mouse secondary antibody. Protein bands were visualized using chemiluminescence and exposure to X-ray film.

**Immunohistochemistry.** Mice were perfused with PBS followed by fixative, 4% paraformaldehyde in PBS, and tissue postfixed with the same solution for 4 h. Whole brains were embedded in paraffin, cut into 20- $\mu$ m sections, mounted onto glass slides, and the paraffin removed. Antigen retrieval was accomplished by microwaving in 1 mM of citrate monohydrate pH 6.0. Endogenous peroxidase activity was quenched with 3% H<sub>2</sub>O<sub>2</sub> in methanol incubation for 5 min at 40 °C. Sections were blocked with 5% normal goat serum and goat anti-mouse Fab fragment (1:250) (Jackson ImmunoResearch) diluted in Tris-Saline Brij, pH 7.5, and incubated in primary anti-RGS14 monoclonal antibody (NeuroMabs) overnight at 4 °C. Sections were then washed and incubated in biotinylated goat anti-mouse secondary antibody (BA-9200; Vector Labs) followed by avidin-biotin-peroxidase complex (Vectastain Elite ABC kit) and developed with 3,3'-diaminobenzidine (DAB substrate kit, SK-4100; Vector Labs). Nuclei were counterstained with hematoxylin. For preadsorption, pure thyoedoxin-his-tagged RGS14 was incubated with anti-RGS14 antibody at a protein ratio of 10 to 1 for overnight at 4 °C.

**Electron Microscopy (EM).** Mice were transcardially perfused with Ringer's solution followed by a fixative containing 4% paraformaldehyde and 0.1% glutaraldehyde in phosphate buffer (0.1 M; pH 7.4). Tissue was cut, labeled using preembedding immunoperoxidase staining with RGS14 monoclonal antibody, and prepared for EM as described (45). Sections were examined on the Zeiss EM-10C electron microscope. Electron micrographs were taken and saved with a CCD camera (DualView 300W; Gatan) controlled by Digital Micrograph software (version 3.10.1; Gatan).

**Hippocampal Slice Preparation.** Hippocampal slices were prepared from RGS14-KO and WT mice (CA2: postnatal days 14–18, CA1: 8–12 wk) as described (7). Animals were decapitated, and the brains rapidly removed. Coronal brain slices (340–400  $\mu$ m thick) containing the hippocampus were cut using a vibrating blade microtome in aerated, ice-cold artificial cerebral spinal fluid (ACSF). Freshly cut slices were allowed to recover for at least 1 h in ACSF at room temperature and were then transferred to a recording chamber in which they were bathed continuously with room temperature ACSF.

**Whole-Cell Patch Recordings.** Recordings were made from individual CA2 neurons due to the difficulty in localizing CA2 dendrites, which makes assessment of field potentials unreliable. Recordings of CA2 neurons were made with patch pipettes (4–6 M $\Omega$ ) only when the CA2 could be visually distinguished from neighboring regions CA1 and CA3. Cluster-type stimulating electrodes (FHC) were placed in the stratum radiatum  $\approx$ 150  $\mu$ m from the patched neuron to stimulate the Schaffer collateral axons and measure excitatory postsynaptic currents (EPSCs) (24). Neuronal excitability was examined by recording the response of each neuron to depolarizing current steps in current clamp mode (0.1–0.6  $\mu$ A), measurement of input resistance, and by recording action potentials in response to 1 s of 100 Hz (LTP-inducing) synaptic stimulation. Action potential threshold was identified using previously published mathematical methods (46). Electrically evoked synaptic responses were recorded at –70 and +40 mV in ACSF containing 1 mM gabazine for measurement of NMDA- and AMPA-type synaptic currents (47).

**Field Potential Recordings.** Extracellular field potential recordings in the stratum radiatum area of CA1 were recorded in response to Schaffer collateral inputs. Population excitatory postsynaptic potential (EPSP) output was measured in response to varying input currents to determine baseline synaptic transmission. For induction of LTP, WT and RGS14-KO hippocampal slices were prepared and maintained as described above. Slices were then subjected to stimulation (2  $\times$  1 s, 100 Hz, 20-s intervals) to induce LTP and postsynaptic neurotransmission was monitored every 15 s for 180 min. Data presented are pooled mean  $\pm$  SD.

**Novel Object Recognition.** The object recognition apparatus consisted of an open box (44  $\times$  44  $\times$  8 cm) made of white PVC placed in a sound-isolated testing room. Four objects ( $\approx$ 7 cm height and 6 cm diameter) made of a combination of plastic, metal, and rubber were used in this task. The weight of the objects ensured that they could not be displaced by mice. Training and testing sessions were recorded with a video camera mounted over the training arena and analyzed using LimeLight video-tracking software (Coulbourn). Novel object recognition tests were carried out as described (48). Time

exploring and number of contacts for each object were expressed as percentages of total time or number of contacts.

**Morris Water Maze.** Adult RGS14-KO and WT littermates ages 2–6 mo were used. The water maze consisted of a circular swim arena (diameter of 116 cm, height of 75 cm) surrounded by extramaze visual cues that remained in the same position for the duration of training and filled to cover the platform by 1 cm at 22 °C. Water was made opaque with nontoxic, white tempera paint. The escape platform was a circular, nonskid surface (area 127 cm<sup>2</sup>) placed in the NW quadrant of the maze. Acquisition training consisted of 5 test d with four daily trials. Mice entered the maze facing the wall and began each trial at a different entry point in a semirandom order. Trials lasted 60 s or until the animal mounted the platform with a 15-min intertrial interval. A probe trial was conducted on day 6 wherein the platform was removed, and the animal swam for 60 s and the time spent in the target quadrant (NW) versus the adjacent and opposite quadrants was recorded. A video camera mounted above the swim arena and linked to TopScan software recorded swim distance, swim

speed and time to platform and was used for tracking and analysis. Statistics were ANOVA and post hoc Dunnett's test unless otherwise stated.

**ACKNOWLEDGMENTS.** We thank Susan Campbell and Jing Wang for technical assistance with electrophysiological studies of CA1 hippocampus and Susan Jenkins and Jean-Francois Pare for technical assistance with the electron microscopy immunocytochemistry experiments. This work was supported by National Institutes of Health Grants R01 NS037112 and R01 NS049195 (to J.R.H.), Grant R01 DA017963 (to D.W.), Grant R01 DA019624 and the Burroughs Wellcome Fund (to K.J.R.), the Yerkes Primate Center Base Grant RR00165 (to Y.S.), Emory National Institute of Neurological Disorders and Stroke Neuroscience Core Facilities Grant P30 NS055077, Training Grant 5 T32 GM008602 to the Emory Molecular and Systems Pharmacology graduate program, and the National Institutes of Health Neuroscience Blueprint Core Grant P30 NS57098 (to J.D.S.). This research was supported in part by the Intramural Research Program of the National Institutes of Health, National Institute of Environmental Health Sciences (Z01 ES100221, to S.M.D.). Monoclonal antibodies were generated in collaboration with the University of California-Davis/National Institutes of Health NeuroMab Facility, and RGS14-KO mice were generated and made available by the NIH Mutant Mouse Regional Resource Center/Lexicon Genetics.

- Neves G, Cooke SF, Bliss TVP (2008) Synaptic plasticity, memory and the hippocampus: A neural network approach to causality. *Nat Rev Neurosci* 9:65–75.
- Nakazawa K, et al. (2003) Hippocampal CA3 NMDA receptors are crucial for memory acquisition of one-time experience. *Neuron* 38:305–315.
- Rolls ET, Kesner RP (2006) A computational theory of hippocampal function, and empirical tests of the theory. *Prog Neurobiol* 79:1–48.
- Woodhams PL, Celio MR, Ulfing N, Witter MP (1993) Morphological and functional correlates of borders in the entorhinal cortex and hippocampus. *Hippocampus* 3 (Spec No):303–311.
- Ishizuka N, Cowan WM, Amaral DG (1995) A quantitative analysis of the dendritic organization of pyramidal cells in the rat hippocampus. *J Comp Neurol* 362:17–45.
- Lein ES, Callaway EM, Albright TD, Gage FH (2005) Redefining the boundaries of the hippocampal CA2 subfield in the mouse using gene expression and 3-dimensional reconstruction. *J Comp Neurol* 485:1–10.
- Zhao M, Choi YS, Obrietan K, Dudek SM (2007) Synaptic plasticity (and the lack thereof) in hippocampal CA2 neurons. *J Neurosci* 27:12025–12032.
- Simons SB, Escobedo Y, Yasuda R, Dudek SM (2009) Regional differences in hippocampal calcium handling provide a cellular mechanism for limiting plasticity. *Proc Natl Acad Sci USA* 106:14080–14084.
- Kirino T (1982) Delayed neuronal death in the gerbil hippocampus following ischemia. *Brain Res* 239:57–69.
- Sadowski M, et al. (1999) Pattern of neuronal loss in the rat hippocampus following experimental cardiac arrest-induced ischemia. *J Neurol Sci* 168:13–20.
- Benes FM, Kwok EW, Vincent SL, Todtenkopf MS (1998) A reduction of nonpyramidal cells in sector CA2 of schizophrenics and manic depressives. *Biol Psychiatry* 44:88–97.
- Kennedy MB, Beale HJ, Carlisle HJ, Washburn LR (2005) Integration of biochemical signalling in spines. *Nat Rev Neurosci* 6:423–434.
- Ross EM, Wilkie TM (2000) GTPase-activating proteins for heterotrimeric G proteins: Regulators of G protein signaling (RGS) and RGS-like proteins. *Annu Rev Biochem* 69:795–827.
- Hollinger S, Hepler JR (2002) Cellular regulation of RGS proteins: modulators and integrators of G protein signaling. *Pharmacol Rev* 54:527–559.
- Snow BE, Antonio L, Suggs S, Gutstein HB, Siderovski DP (1997) Molecular cloning and expression analysis of rat Rgs12 and Rgs14. *Biochem Biophys Res Commun* 233:770–777.
- Traver S, et al. (2000) RGS14 is a novel Rap effector that preferentially regulates the GTPase activity of G alpha o. *Biochem J* 350:19–29.
- Cho H, Kozasa T, Takekoshi K, De Gunzburg J, Kehrl JH (2000) RGS14, a GTPase-activating protein for G1alpha, attenuates G1alpha- and G13alpha-mediated signaling pathways. *Mol Pharmacol* 58:569–576.
- Hollinger S, Taylor JB, Goldman EH, Hepler JR (2001) RGS14 is a bifunctional regulator of Galphai/o activity that exists in multiple populations in brain. *J Neurochem* 79:941–949.
- Traver S, Spingard A, Gaudriault G, De Gunzburg J (2004) The RGS (regulator of G-protein signalling) and GoLoco domains of RGS14 co-operate to regulate Gi-mediated signalling. *Biochem J* 379:627–632.
- Kimple RJ, et al. (2001) RGS12 and RGS14 GoLoco motifs are G alpha(i) interaction sites with guanine nucleotide dissociation inhibitor Activity. *J Biol Chem* 276:29275–29281.
- Shu FJ, Ramineni S, Hepler JR (2010) RGS14 is a multifunctional scaffold that integrates G protein and Ras/Raf MAPkinase signalling pathways. *Cell Signal* 22:366–376.
- Bliss TVP, Collingridge GL (1993) A synaptic model of memory: Long-term potentiation in the hippocampus. *Nature* 361:31–39.
- Shu FJ, Ramineni S, Amyot W, Hepler JR (2007) Selective interactions between Gi alpha1 and Gi alpha3 and the GoLoco/GPR domain of RGS14 influence its dynamic subcellular localization. *Cell Signal* 19:163–176.
- English JD, Sweatt JD (1997) A requirement for the mitogen-activated protein kinase cascade in hippocampal long term potentiation. *J Biol Chem* 272:19103–19106.
- Cohen-Matsliah SI, Brosh I, Rosenblum K, Barkai E (2007) A novel role for extracellular signal-regulated kinase in maintaining long-term memory-relevant excitability changes. *J Neurosci* 27:12584–12589.
- Mark MD, Herlitze S (2000) G-protein mediated gating of inward-rectifier K+ channels. *Eur J Biochem* 267:5830–5836.
- Lei Q, Jones MB, Talley EM, Garrison JC, Bayliss DA (2003) Molecular mechanisms mediating inhibition of G protein-coupled inwardly-rectifying K+ channels. *Mol Cells* 15:1–9.
- Yuan L-L, Adams JP, Swank M, Sweatt JD, Johnston D (2002) Protein kinase modulation of dendritic K+ channels in hippocampus involves a mitogen-activated protein kinase pathway. *J Neurosci* 22:4860–4868.
- Ennaceur A, Delacour J (1988) A new one-trial test for neurobiological studies of memory in rats. 1: Behavioral data. *Behav Brain Res* 31:47–59.
- López-Aranda MF, et al. (2009) Role of layer 6 of V2 visual cortex in object-recognition memory. *Science* 325:87–89.
- Vorhees CV, Williams MT (2006) Morris water maze: procedures for assessing spatial and related forms of learning and memory. *Nat Protoc* 1:848–858.
- DeVito LM, et al. (2009) Vasopressin 1b receptor knock-out impairs memory for temporal order. *J Neurosci* 29:2676–2683.
- Malenka RC, Bear MF (2004) LTP and LTD: An embarrassment of riches. *Neuron* 44:5–21.
- Zhu Y, et al. (2005) Rap2-JNK removes synaptic AMPA receptors during depotentiation. *Neuron* 46:905–916.
- Manabe T, et al. (2000) Regulation of long-term potentiation by H-Ras through NMDA receptor phosphorylation. *J Neurosci* 20:2504–2511.
- Zhu JJ, Qin Y, Zhao M, Van Aelst L, Malinow R (2002) Ras and Rap control AMPA receptor trafficking during synaptic plasticity. *Cell* 110:443–455.
- Pineda VV, et al. (2004) Removal of G(alpha1) constraints on adenylyl cyclase in the hippocampus enhances LTP and impairs memory formation. *Neuron* 41:153–163.
- Kushner SA, et al. (2005) Modulation of presynaptic plasticity and learning by the H-ras/extracellular signal-regulated kinase/synapsin I signaling pathway. *J Neurosci* 25:9721–9734.
- Tada T, Sheng M (2006) Molecular mechanisms of dendritic spine morphogenesis. *Curr Opin Neurobiol* 16:95–101.
- Fu Z, et al. (2007) Differential roles of Rap1 and Rap2 small GTPases in neurite retraction and synapse elimination in hippocampal spiny neurons. *J Neurochem* 100:118–131.
- Ryu J, Futai K, Feliu M, Weinberg R, Sheng M (2008) Constitutively active Rap2 transgenic mice display fewer dendritic spines, reduced extracellular signal-regulated kinase signaling, enhanced long-term depression, and impaired spatial learning and fear extinction. *J Neurosci* 28:8178–8188.
- Bourtchuladze R, et al. (1994) Deficient long-term memory in mice with a targeted mutation of the cAMP-responsive element-binding protein. *Cell* 79:59–68.
- Blazer LL, Neubig RR (2009) Small molecule protein-protein interaction inhibitors as CNS therapeutic agents: current progress and future hurdles. *Neuropsychopharmacology* 34:126–141.
- Lee YS, Silva AJ (2009) The molecular and cellular biology of enhanced cognition. *Nat Rev Neurosci* 10:126–140.
- Mitrano DA, Arnold C, Smith Y (2008) Subcellular and subsynaptic localization of group I metabotropic glutamate receptors in the nucleus accumbens of cocaine-treated rats. *Neuroscience* 154:653–666.
- Henze DA, González-Burgos GR, Urban NN, Lewis DA, Barrionuevo G (2000) Dopamine increases excitability of pyramidal neurons in primate prefrontal cortex. *J Neurophysiol* 84:2799–2809.
- Myme CIO, Sugino K, Turrigiano GG, Nelson SB (2003) The NMDA-to-AMPA ratio at synapses onto layer 2/3 pyramidal neurons is conserved across prefrontal and visual cortices. *J Neurophysiol* 90:771–779.
- Heldt SA, Stanek L, Chhatwal JP, Ressler KJ (2007) Hippocampus-specific deletion of BDNF in adult mice impairs spatial memory and extinction of aversive memories. *Mol Psychiatry* 12:656–670.